Geological Quarterly, 2020, **64** (2): 263–274
DOI: http://dx.doi.org/10.7306/gq.1529

$Cu_3(As,Sb)S_4$ minerals from the Baia Mare metallogenic district, Eastern Carpathians, Romania – a case study from the Cisma ore deposit

Réka KOVÁCS[1, 2] and Călin Gabriel TĂMAŞ[1, *]

[1] Babeş-Bolyai University, Faculty of Biology and Geology, Department of Geology, 1 Mihail Kogălniceanu street, 400084 Cluj-Napoca, Romania

[2] Victor Gorduza County Mineralogical Museum of Baia Mare, 8 Traian boulevard, 430212 Baia Mare, Romania

Kovács, R., Tămaş, C.G., 2020. $Cu_3(As,Sb)S_4$ minerals from the Baia Mare metallogenic district, Eastern Carpathians, Romania – a case study from the Cisma ore deposit. Geological Quarterly, **64** (2): 263–274, doi: 10.7306/gq.1529

Associate Editor: Sławomir Oszczepalski

The occurrence of $Cu_3(As,Sb)S_4$ minerals, i.e. the enargite and luzonite-famatinite series, is poorly known in the Neogene Baia Mare metallogenic district, NW Romania, with few records and no analytical data. This study provides the first EPMA and XRD data on enargite/luzonite from the Baia Mare metallogenic district, i.e. the Cisma ore deposit from the Băiuţ metallogenic field, and the Herja ore deposit. Vein-type ore bodies bearing $Cu_3(As,Sb)S_4$ minerals from Cisma are hosted by Paleocene–Eocene flysch successions, while the host rock of the enargite-bearing ore from Herja is unknown. The enargite and luzonite–famatinite series are known as "exotic" in low sulphidation epithermal ore deposits, "typical" in high sulphidation epithermal deposits in association with tennantite, and "sometimes common" in small amounts in intermediate sulphidation epithermal ore deposits. The occurrence of enargite/luzonite in the Baia Mare district suggests the need to update the metallogenic interpretation for several ore deposits, partly at the district scale in relation to other ore deposit/mineralogy features, e.g. vuggy silica, hypogene argillic alteration.

Key words: enargite, luzonite, Cisma, Băiuţ, Herja, Baia Mare metallogenic district.

INTRODUCTION

According to many authors (e.g., Mariaş, 1996, 2005; Grancea et al., 2002; Marcoux et al., 2002; Kouzmanov et al., 2005), the Baia Mare metallogenic district, Romania (Fig. 1A and B) consists of typical low-sulphidation epithermal ore deposits. This interpretation is based on early mention of adularia alteration at the district scale by Giuşcă (1960) and Lang et al. (1994), the widespread occurrence of carbonates (e.g., Lang, 1979), the minor occurrence of covellite, and the absence from the ores of enargite, and luzonite-famatinite. However, Kovács-Pálffy et al. (1977) described a high-sulphidation-like alteration mineral assemblage with pyrite associated with alunite in the Ilba-Nistru area. Minor adularia and frequent propylitization, sericitization and argillization were reported by Stanciu (1973) in ore deposits from the central and eastern Baia Mare district (Dealul Crucii to Băiuţ deposits), while chlorite-adularia-sericite-argillic (locally carbonate and silicic) alteration was mentioned by Stanciu (1984) in the southern part of the Gutâi Mountains. A quartz-illite-kaolinite-pyrophyllite assemblage was described by Mariaş (2005) in the central part of the Cavnic ore deposit (Bolduţ mine), which may be interpreted as transitional from sericitic to argillic alteration. Finally, in the upper part of the Cavnic ore deposit a kaolinite±pyrophyllite±alunite assemblage was mentioned by Mariaş (1996).

The present study offers the first EPMA and XRD data on enargite from the Baia Mare metallogenic district. Enargite (Cu_3AsS_4) is a sulphide (Takéuchi and Sadanaga, 1969) with orthorhombic hexagonal close-packed structure. It is a polytype of luzonite, which together with famatinite are the end-members of a tetragonal, cubic close-packed complete solid solution series between Cu_3AsS_4 and Cu_3SbS_4 (Gaines, 1957; Pósfai and Buseck, 1998). As shown by Pósfai and Sundberg (1998) and Pósfai and Buseck (1998) the enargite and luzonite-famatinite series are frequently intergrown at the atomic level. Enargite (Cu_3AsS_4) is commonly used as an indicator of the sulphidation state of sulphide assemblages in epithermal deposits. Enargite is considered "exotic" in low-sulphidation (LS) epithermal ore deposits (Hedenquist et al., 1994), while, abundantly associated with tennantite and pyrite, it is typical of high-sulphidation (HS), and in smaller amounts of intermediate-sulphidation (IS) epithermal ore deposits (Einaudi et al., 2003).

* Corresponding author, e-mail: calingtamas@yahoo.fr

Received: July 22, 2019; accepted: January 31, 2020; first published online: April 23, 2020

REGIONAL GEOLOGY

The Carpathian chain is situated in the central-eastern part of Europe and is part of the Carpathian–Pannonian area that is formed of two microplates, Alcapa and Tisia, which are separated by the "Mid-Hungarian Line", a major transcrustal fault (Csontos and Nagymarosy, 1998). The Alcapa and the Tisia microplates underwent different tectonic evolution during Mesozoic and Cenozoic, i.e. with opposite rotations during the Neogene (Csontos et al., 1992; Csontos, 1995; Seghedi et al., 1998), and with different translations (Márton et al., 1992; Pătraşcu et al., 1994; Panaiotu et al., 1996). During the Early to Middle Miocene the Tisia microplate translated eastwards along the Alcapa microplate (Csontos, 1995; Fodor et al., 1999; Huismans et al., 2001).

Neogene–Quaternary volcanic activity took place within the Carpathian–Pannonian region and it occurred on both Alcapa and Tisia microplates as a volcanic chain located in the inner part of the Eastern Carpathians. This volcanic arc is the result of subduction, collision, post-collisional and extensional processes among European and Alcapa–Tisia plates (Seghedi and Downes, 2011). The volcanism started in the Western Carpathians and Pannonian Basin with Early Miocene felsic calc-alkaline volcanism (21–18 Ma), which was followed by Middle Miocene–Pliocene felsic and intermediate calc-alkaline volcanism (18–8 Ma) and ended during the Pliocene-Pleistocene with alkaline basaltic volcanism (10–0.1 Ma; Szabó et al., 1992; Seghedi et al., 2005). Calc-alkaline volcanism was active in the westernmost part of the Eastern Carpathians between 15–9 Ma, while in the Apuseni Mountains area it started as adakitic calc-alkaline volcanism between 15 – 9 Ma and ended with OIB-like alkali basaltic (2.5 Ma) and shoshonitic (1.6 Ma) volcanism (Seghedi et al., 2005).

GUTÂI MOUNTAINS

The Gutâi Mountains comprises an important segment of the Neogene–Quaternary volcanic arc of the Eastern Carpathians, located at the northeastern margin of Alcapa and Tisia microplates (Grancea et al., 2002). The Gutâi Mts. are composed of three main geological units: (1) the pre-volcanic basement; (2) the Neogene sedimentary cover; and (3) the Neogene volcanic rocks (Săndulescu, 1984). The pre-volcanic basement consists of Precambrian/Paleozoic metamorphic rocks and Cretaceous to Oligocene flysch deposits (Săndulescu, 1984; Săndulescu et al., 1993). The Neogene sedimentary cover is composed of Badenian/Kosovian (mudstones), Sarmatian/Volhynian–Bessarabian (mudstones, siltstones, sandstones) and Pannonian (mudstones, siltstones, sandstones, microconglomerates, coals) deposits, which formed more or less synchronously with the volcanic activity (Kovacs and Fülöp, 2010). The Neogene sedimentary rocks are overlain by the Neogene volcanic rocks across almost the entire district (Kovacs and Fülöp, 2010).

Neogene volcanic activity in the Gutâi Mountains started in the Badenian (15.4 Ma; Fülöp, 2001) with silicic calc-alkaline extensional volcanism (Fülöp and Kovacs, 2003), composed of rhyolitic ignimbrites, fallout tuffs and resedimented volcaniclastic rocks in the southwestern part of the area (Fülöp, 2003). The silicic calc-alkaline volcanism was followed by intermediate calc-alkaline arc-type volcanism, which started in the Sarmatian (13.4 Ma; Edelstein et al., 1992), and continued southwards until the Quaternary (<0.1 Ma) along the entire Eastern Carpathian chain (Pécskay et al., 2006). The main volcanic structures in the Gutâi Mountains and Eastern Carpathians formed during the intermediate volcanism. The surface volcanic rocks that belong to the intermediate volcanism in the Gutâi Mountains consist of basalts, pyroxene basaltic andesites, dacites and rhyolites (Kovacs and Fülöp, 2003), while at subvolcanic level gabbros, diorites, microdiorites, monzodiorites and microgranodiorites have been identified (Fülöp and Kovacs, 2003). The intermediate calc-alkaline volcanic activity in the Gutâi Mountains triggered important metallogenic activity.

BAIA MARE METALLOGENIC DISTRICT

The Baia Mare metallogenic district in the Eastern Carpathian volcanic chain is located in the Gutâi Mountains (Fig. 1B). The ore deposits in this district are structurally controlled by the E–W striking Bogdan Vodă–Dragoş Vodă fault system (Neubauer et al., 2005) located along the southern part of the Gutâi Mountains; this fault is considered the easternmost prolongation of the "Mid-Hungarian Line" (Csontos and Nagymarossy, 1998; Tischler et al., 2007). According to mining and drilling data, satellite images and gravity anomalies, the fault is partly hidden by Neogene volcanic rocks (Săndulescu et al., 1993; Grancea et al., 2002); however, it is well exposed in the eastern part of the Baia Mare ore district (Grancea et al., 2002). The magmatic control on the ore deposits consists of a pluton, which according to geophysical and drilling data (Borcoş, 1994; Crahmaliuc et al., 1995; Bailly et al., 1998) is located along the southern part of the Gutâi Mountains (Fig. 1B).

The Baia Mare metallogenic district has been divided in three metallogenic sub-districts (Fig. 1B), from west to east as follows: (1) Ilba–Nistru (Pb-Zn-Cu±Au, Ag); (2) Săsar–Dealul Crucii (Au, Ag); (3) Herja–Băiuţ (Pb-Zn-Cu and Au-Ag; Kovacs and Fülöp, 2010).

The ore deposits in the Baia Mare district are genetically linked to the intermediate calc-alkaline volcanism (Iancu and Kovacs, 2010) and are considered by many authors as of low-sulphidation type (e.g., Grancea et al., 2002; Mariaş, 2005), or as transitional between low- and high-sulphidation (Mârza, 2002). The ore bodies occur mainly as vein structures and subordinately as stockworks, breccia dykes and breccia pipes (Gurău et al., 1970; Marcoux et al., 2002; Kouzmanov et al., 2005; Iancu and Kovacs, 2010), which together show clear geochemical vertical zoning (Manilici et al., 1965; Marcoux et al., 2002; Mârza, 2002; Mariaş, 2005).

At the scale of the Baia Mare metallogenic district Bailly et al. (1998) and Grancea et al. (2002) distinguished five ore deposition stages as follows: (1) Fe with hematite–magnetite±wolframite±scheelite; (2) Cu-Bi-(W) with chalcopyrite–pyrite–covellite–bismuth sulphides and sulphosalts and rare gold; (3) Pb-Zn with sphalerite–galena–chalcopyrite–tetrahedrite–tennantite±gold in quartz–adularia–illite/smectite–rhodonite–calcite–kutnohorite and rhodochrosite gangue; (4) Sb with bournonite–tetrahedrite–stibnite with subordinate gold and rare realgar and orpiment; and (4) Au-Ag with gold–proustite/pyrargyrite–pearceite/polybasite–native arsenic.

Radiometric data by Lang et al. (1994) and Kovacs et al. (1997) indicate that the overall age of the hydrothermal activity in the Baia Mare ore district is Pannonian (11.5–7.9 Ma). According to these authors the ore deposits in the Ilba–Nistru and Săsar–Dealul Crucii metallogenic sub-districts are of Early Pannonian age (11.5–10.0 Ma), while the ore deposits in Herja-Băiuţ metallogenic sub-district are Late Pannonian (9.4–7.9 Ma). The ore deposit age progression from west to

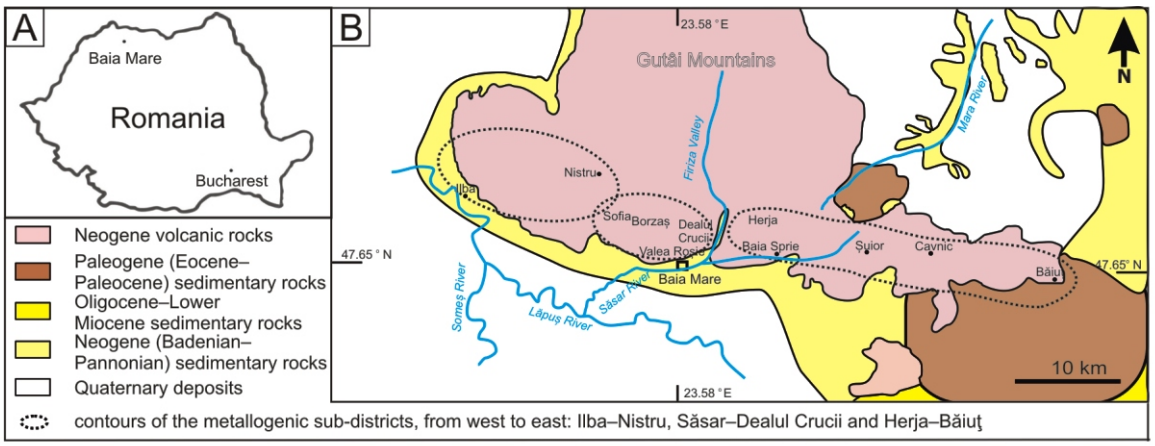

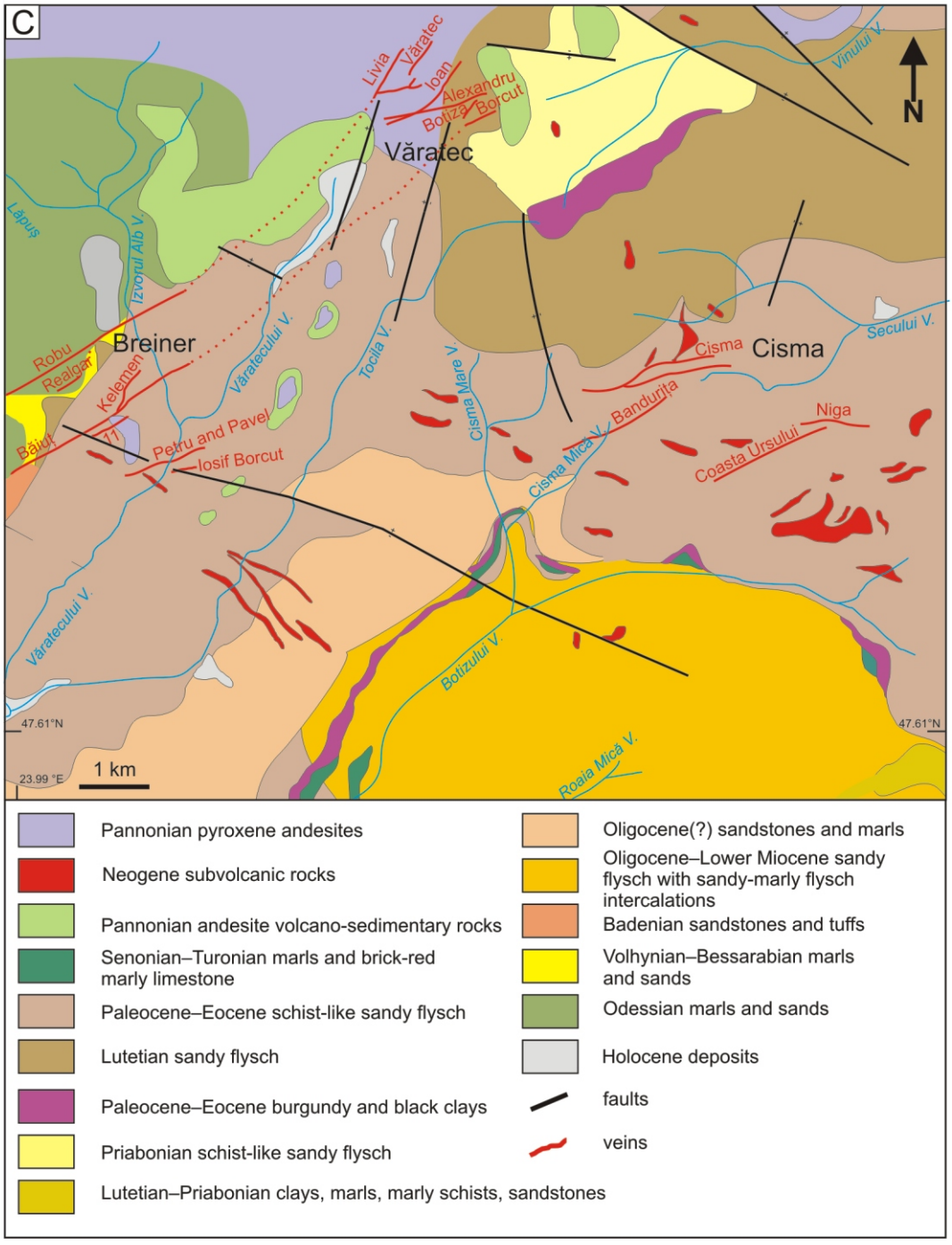

Fig. 1. Location and geology of the area studied

A – position of the Baia Mare metallogenic district in Romania; **B** – simplified map of the Baia Mare metallogenic district in the Gutâi Mountains (modified after Kovacs and Fülöp, 2010; Kovacs et al., 2017); **C** – simplified geological map of the Băiuţ metallogenic field (modified after Săndulescu and Russo-Săndulescu, 1981; Kovacs et al., 1997; Mariaş, 2005)

east follows the volcanism age progression (Lang, 1979) with an ~1 Ma gap between volcanism and ore deposition (Mariaş, 2005).

BĂIUŢ METALLOGENIC FIELD

The Băiuţ metallogenic field is situated in the easternmost part of the Herja-Băiuţ metallogenic sub-district and is composed of three main ore deposits (Fig. 1C), (from west to east): Breiner–Băiuţ, Văratec and Cisma–Poiana Botizei (Borcoş and Gheorghiţă, 1976). According to available mineralogical data, the Băiuţ metallogenic field has been considered during the last few decades as a meso-hypothermal deposit by Lang (1979), and as a low-sulphidation epithermal gold-polymetallic ore deposit by Grancea et al. (2002) and Mariaş (2005).

CISMA–POIANA BOTIZEI ORE DEPOSIT

The Cisma–Poiana Botizei (Cisma) deposit is easternmost in the Baia Mare metallogenic district (Fig. 1C), together with the Băiuţ metallogenic field. It comprises the Cisma, Banduriţa (Borcoş and Gheorghiţă, 1976; Istvan et al., 1995; Damian et al., 2016), Prisăcele, Coasta Ursului, Niga, and Olimpiu veins (Edelstein et al., 1992; Mariaş, 2005). These veins are hosted by Paleocene–Eocene schist-like sandy flysch (Săndulescu and Russo-Săndulescu, 1981), which is intruded by Neogene quartz microdiorite and microgranodiorite porphyries (Plotinskaya et al., 2012). Two mineralization stages were identified by Damian and Damian (2004). The first stage is composed of hematite, pyrite, chalcopyrite, tennantite, and tetrahedrite (dominant), and sphalerite, galena, wolframite and pyrrhotite, together with several mineral compositions of the lillianite–gustavite series, and native Bi (subordinate). The second stage contains galena, sphalerite, pyrite, chalcopyrite, marcasite, native gold, stibnite, realgar, orpiment, semseyite, boulangerite and jamesonite. The veins are mostly massive with some related disseminations.

HERJA ORE DEPOSIT

The Herja ore deposit is located in the central part of the Baia Mare metallogenic district, ~8 km NE from the Baia Mare. It is a Pb, Zn, Ag, Sb and subordinately Au deposit that consists of a vein system including 247 structures mined underground out of >260 known structures (Damian, 1996). The veins are hosted by Eocene mudstones and siltstones, Seravallian and Tortonian sandstones, clays, marls and tuffs, and Tortonian quartz andesites and pyroxene andesite lavas and quartz andesite and microdiorite subvolcanic bodies (Damian, 1996). The ore deposit is the type locality of fizélyite ($Pb_{14}Ag_5Sb_{21}S_{48}$) and is known for well-developed stibnite, a complex sulphosalt assemblage (Damian, 1996; Cook and Damian, 1997; Udubaşa et al., 2002), and the occurrence of black calcite (Tămaş et al., 2018) that occasionally forms black and bi-coloured black and white spheres (Mârza et al., 2019). The deposit was interpreted as of low-sulphidation type by Damian (1996).

PREVIOUS DATA ON ENARGITE AND LUZONITE–FAMATINITE FROM THE BAIA MARE METALLOGENIC DISTRICT

The occurrence of enargite and luzonite–famatinite in the Baia Mare metallogenic district is poorly known and superficially described. Pomârleanu (1971) briefly mentioned the presence of enargite, famatinite and luzonite in the Cavnic ore deposit, while Petrulian et al. (1976) included enargite among the ore minerals of the second paragenetic Sb- and Ag-bearing sequence they proposed for the Cavnic ore deposit, with enargite associated with tetrahedrite, bournonite, stibnite, semseyite, proustite, pyrargyrite, subordinate bismuthinite and germanite. Bailly et al. (1998) placed enargite in the fifth mineralization sequence of the district, which is dominated by electrum, proustite/pyrargyrite, pearceite/polybasite and native As. Damian and Damian (2004) compiled a synthesis of the ore mineralogy in the Baia Mare metallogenic district based on four references, i.e. Cădere (1925), Rădulescu and Dimitrescu (1965), Udubaşa et al. (1992) and Damian et al. (1995), and reported enargite at Nistru (Ilba–Nistru sub-district) and Băiuţ (Herja–Băiuţ sub-district). However, none of these four publications reported the occurrence of enargite at Nistru and Băiuţ or elsewhere in the Baia Mare metallogenic district. András (2017) made the first mention of enargite in the Băiuţ area based on optical microscopy, and subsequently Kovács and Tămaş (2017) confirmed it by SEM-EDS data.

MATERIALS AND METHODS

The new mineralogical data on enargite from the Baia Mare metallogenic district were acquired from ore samples from the Băiuţ and Herja ore deposits by optical microscopy, X-Ray powder diffraction (XRD), scanning electron microscopy (SEM-EDS), and electron probe microanalyzer (EPMA). The samples from Băiuţ (Fig. 2A, B) were collected from the former ore stockpile of the Cisma ore deposit, located in the vicinity of the abandoned Băiuţ processing plant. A sample from Herja (Fig. 2C, D), specimen no. 2660 from the County Museum of Mineralogy Victor Gorduza, Baia Mare, Romania, was also investigated.

The optical microscopy was done using a *Nikon Eclipse LV100N POL* polarizing microscope from Géosciences Environnement Toulouse - Observatoire Midi-Pyrénées (GET), Toulouse, France. The X-Ray diffraction determinations were performed using a *Bruker D8 Advance* diffractometer with Cu K radiation (= 1.5418 Å), *LynxEye* one-dimensional detector and Fe 0.01 mm filter at the Department of Geology, Babeş-Bolyai University in Cluj-Napoca, Romania. The working parameters of the X-Ray diffraction were 40 kV and 40 mA. The diffraction data were collected between 5 and 64° 2 with a step interval of 0.02° 2 . The PDF2 database has been used for mineral identification.

The SEM observations were carried out using a *JSM-6360* electron microscope with 20 kV voltage at the GET Laboratory, Toulouse, France. The quantitative microprobe analyses were made at the Centre de Microcaractérisation Raimond Castaing, Institut National des Sciences Appliquées de

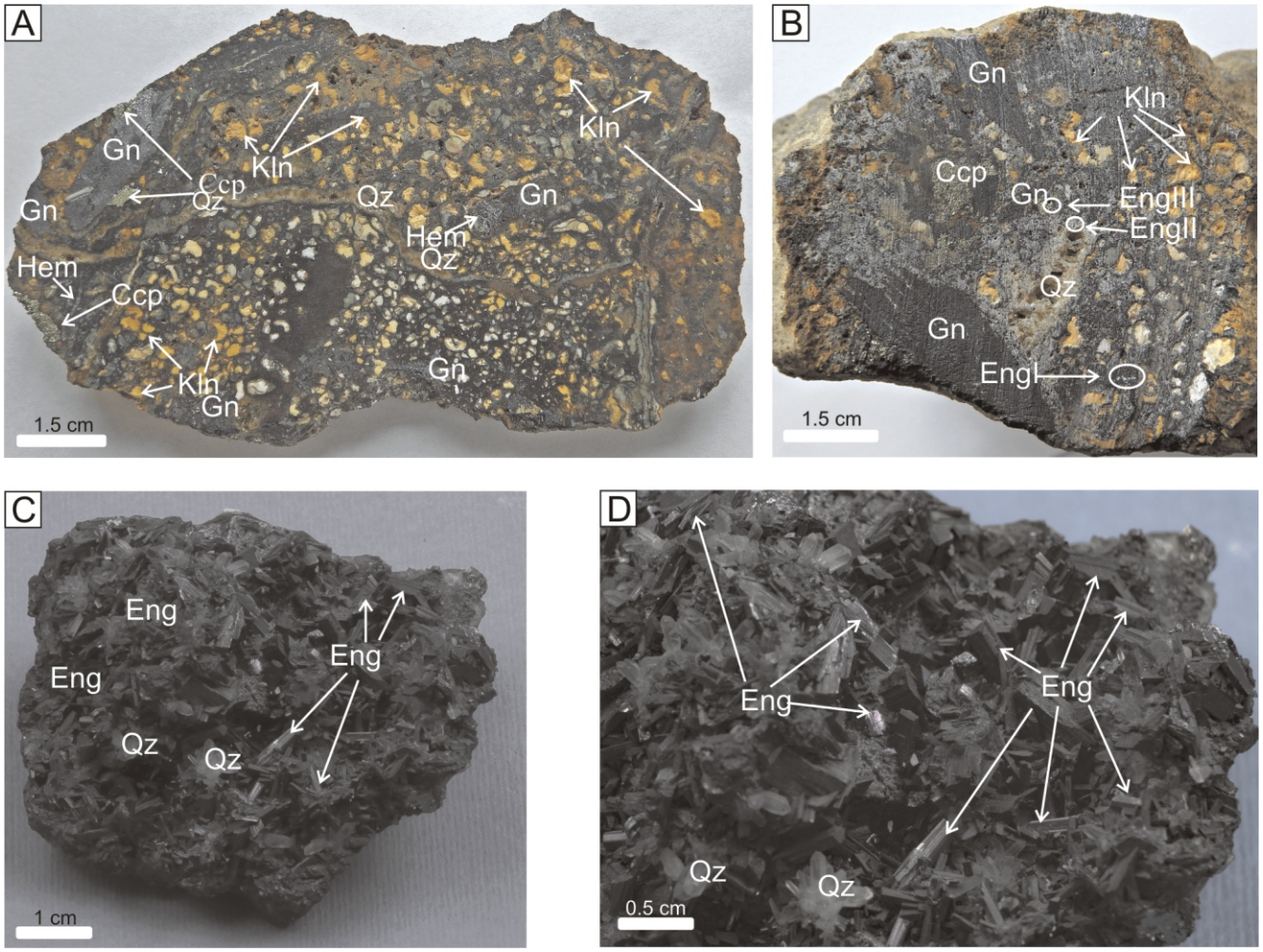

Fig. 2. Enargite-bearing samples from the Baia Mare metallogenic district

A – longitudinal slice of an ore sample from Cisma hosting chalcopyrite, hematite, galena, kaolinite and quartz used for XRD (kaolinite) and EPMA (enargite) investigations; **B** – transverse slice through the ore sample shown in Figure 2A, showing the location of EPMA points for chalcopyrite and enargite – circles; **C, D** – ore sample showing greyish-black prismatic enargite crystals associated with quartz (photos C and D have been taken by Ioan Bereş, museum curator; D is an enlargement of the portion of the sample shown in C); abbreviations: Ccp – chalcopyrite, Eng – enargite, Gn – galena, Hem – hematite, Kln – kaolinite, Qz – quartz

Toulouse, France, by a *CAMECA SXFive* electron microprobe with 25 kV acceleration, a beam current of 20 nA, a surface of the analysed area of 2 2 micrometers and a counting time of 10 s for peaks and 5 s for background. The following standards and radiations have been used: $CuFeS_2$ for S, Fe and Cu; FeAsS for As; pure Ag for Ag; PbS for Pb; pure Sb for Sb; pure Bi for Bi; ZnS for Zn; $MnTiO_3$ for Mn; Cd for Cd; pure Sn for Sn; K lines for Cu, Fe, S, Zn; L lines for Ag, Cd, Sb, Sn; L lines for As; and M lines for Bi and Pb. The minimum detection limits were 450 ppm for S; 570 ppm for Cu; 1960 ppm for Ag; 650 ppm for Zn; 440 ppm for Fe; 2000 ppm for As; 570 ppm for Sb; 3600 ppm for Pb; 2900 ppm for Bi; 300 ppm for Mn; 470 ppm for Sn; and 600 ppm for Cd.

RESULTS

OPTICAL MICROSCOPY AND SCANNING ELECTRON MICROSCOPY

Reflected light microscopy study of ore samples from the Cisma ore deposit allowed the identification of enargite/luzonite and tetrahedrite-tennantite. These minerals are associated with chalcopyrite, sphalerite, galena and hematite. The gangue is represented mainly by quartz.

Enargite/luzonite (Cu_3AsS_4) is moderately abundant and occurs as large (up to 300 μm) pale brown subhedral to anhedral grains with a greyish-purplish tint that contain chalcopyrite inclusions (Fig. 3A). It shows visible bireflectance in plane polarized light and strong anisotropy under crossed polars (Fig. 3B). Enargite/luzonite is often associated with galena associated with chalcopyrite (Fig. 3B, C) or sphalerite (Fig. 3D) and contains local tennantite inclusions controlled by voids. Chalcopyrite is partly replaced by enargite/luzonite (Fig. 3E). Enargite/luzonite is also associated with large (up to 0.25 mm) sphalerite grains (Fig. 3D).

Minerals from the tetrahedrite–tennantite series ($(Cu,Fe)_{12}(As,Sb)_4S_{13}$) occur frequently as replacement of enargite/luzonite coexisting with galena that is associated with well-developed sphalerite with chalcopyrite inclusions (Fig. 3D, E), and as euhedral grains (up to 30 μm) hosted by enargite/luzonite (Fig. 3B).

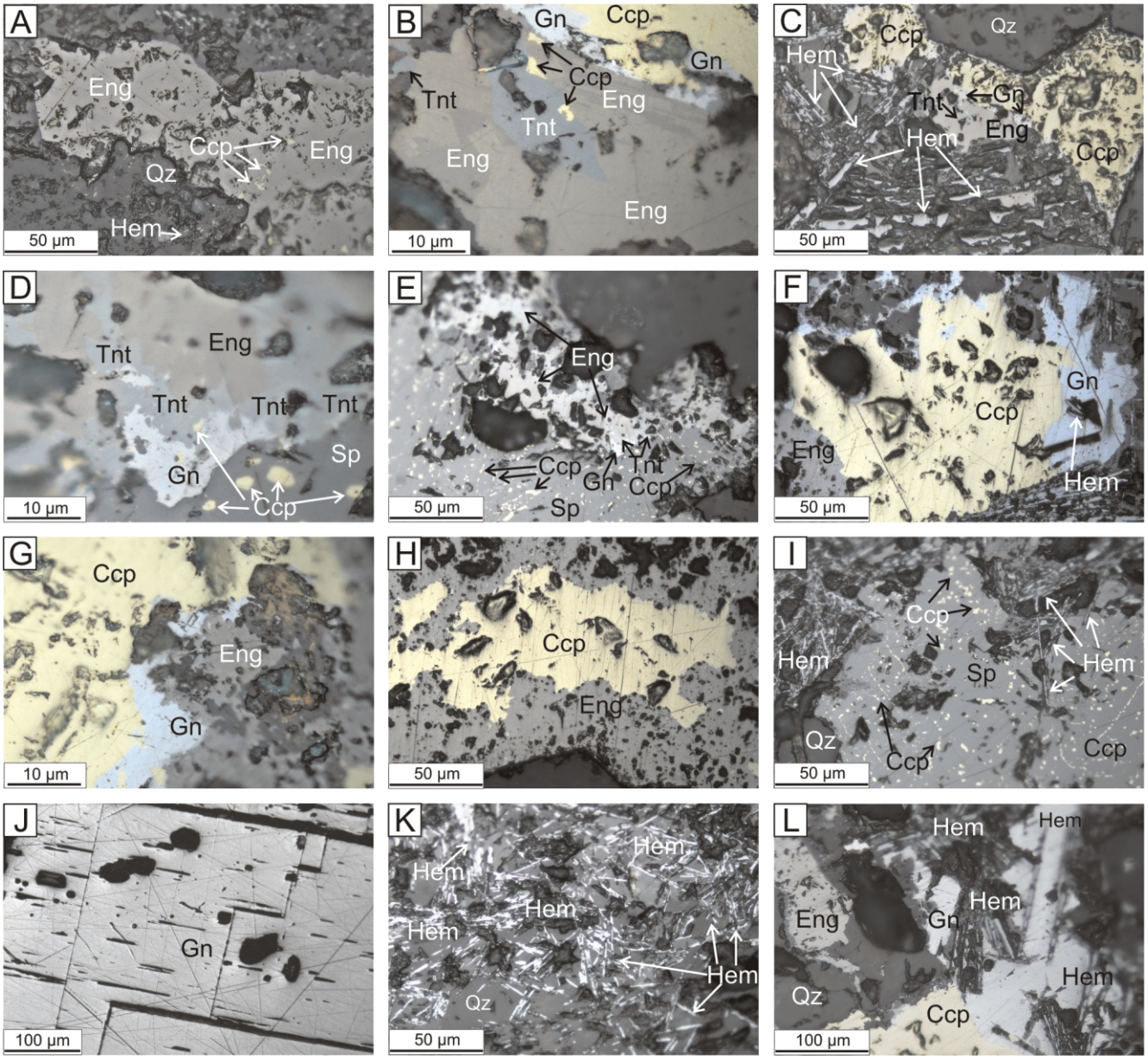

Fig. 3. Reflected light photomicrographs of enargite/luzonite bearing a mineral assemblage from Cisma ore deposit

A – large anhedral enargite/luzonite grain with small chalcopyrite inclusions; **B** – large enargite/luzonite grain with strong anisotropy, showing creamy and purple tints, hosting tennantite-chalcopyrite inclusions and associated with galena and chalcopyrite; **C** – needle-like hematite associated with enargite/luzonite and chalcopyrite; **D** – detail of enargite/luzonite, tennantite and galena associated with sphalerite with chalcopyrite disease; the enargite/luzonite is partly replaced and cut by tennantite; galena is concentrated along the former enargite/luzonite–sphalerite contact; **E** – large sphalerite with chalcopyrite disease associated with enargite/luzonite and subordinate tennantite and galena; **F** – enargite/luzonite, chalcopyrite, and galena hosting a needle-like hematite mineral assemblage; **G** – galena associated with chalcopyrite and enargite/luzonite; **H** – large chalcopyrite grains replaced by enargite/luzonite; note the abundance of voids within enargite/luzonite as compared to chalcopyrite; **I** – thin needle-like hematite crystals associated with later sphalerite with chalcopyrite disease; **J** – galena with triangular pits and visible cleavage; **K** – fibroradial aggregates of hematite hosted by quartz gangue; **L** – enargite and hematite associated with galena and chalcopyrite; abbreviations: Ccp – chalcopyrite, Eng – enargite/luzonite, Gn – galena, Hem – hematite, Qz – quartz, Sp – sphalerite, Tnt – tennantite; A, C–F, H–L in plane polarized light, B and G under crossed polars)

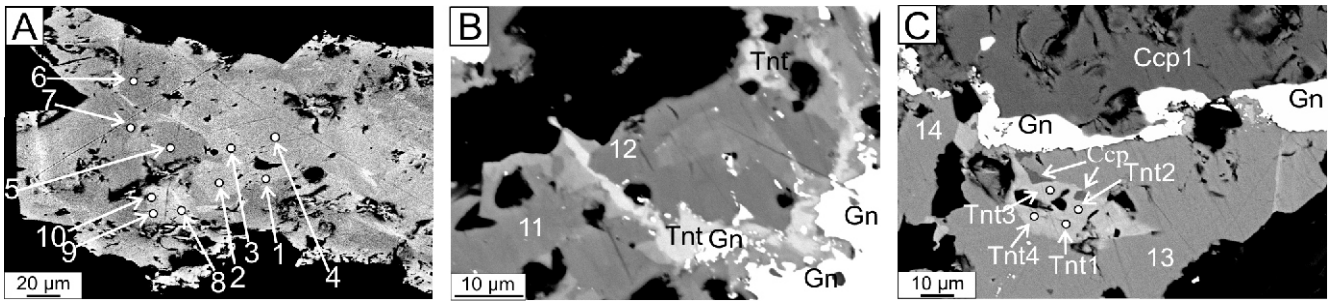

Fig. 4. SEM-BSE images of enargite/luzonite from the Cisma deposit

A – partial view of the large enargite/luzonite grain shown in Figure 3A displaying different shades of grey due to variable amounts of As and Sb; numbers from 1 to 10 indicate the position of EPMA points for enargite/luzonite; **B** – the equivalent SEM-BSE image of Figure 3D with galena, tennantite and enargite/luzonite; numbers 11 and 12 show the location of EPMA points for enargite/luzonite; **C** – the equivalent SEM-BSE image of Figure 3B, with a tennantite-chalcopyrite inclusion in enargite/luzonite associated with galena and chalcopyrite; numbers show the location of EPMA points as follows, 13 and 14 for enargite/luzonite, Tnt1–Tnt4 for tennantite–tetrahedrite, and Ccp1 for chalcopyrite; other explanations as in Figure 3

Large (up to 200 μm) subhedral **chalcopyrite** ($CuFeS_2$) grains are associated with galena (Fig. 3C, F) and enargite/luzonite (Fig. 3G). Chalcopyrite also occurs as large (over 250 μm in length) anhedral inclusions hosted by enargite/luzonite (Fig. 3H). The irregular shape of the contact between chalcopyrite and enargite/luzonite (Fig. 3H) suggests that chalcopyrite was partly replaced by enargite/luzonite. Subhedral to anhedral chalcopyrite grains up to 5 μm in size related to tennantite occur as inclusions in enargite/luzonite (Fig. 3B), as well as in sphalerite showing locally linear distribution (Fig. 3E, I).

Sphalerite occurs as large (up to 250 μm) grains (Fig. 3I), enclosing elongated and rounded chalcopyrite inclusions (Fig. 3I). Subhedral to euhedral sphalerite grains are associated with enargite/luzonite, tennantite, chalcopyrite (Fig. 3E) or galena (Fig. 3D), and locally engulf hematite lamellae (Fig. 3I).

Galena appears as large individual grains showing cleavage and triangular pits (Fig. 3J). It locally marks the contact zone between chalcopyrite and enargite/luzonite (Fig. 3B, G), or between tetrahedrite-tennantite and sphalerite (Fig. 3D). Galena also encircles acicular hematite (Fig. 3F).

Hematite (Fe_2O_3) is abundant within the quartz gangue and appears as elongated lamellae. It may occur as fibroradial aggregates composed of short individual lamellae (Fig. 3K), or as isolated needle-like crystals engulfed by later deposited sulphides, i.e., sphalerite (Fig. 3I), galena (Fig. 3L), chalcopyrite, tetrahedrite–tennantite and enargite/luzonite (Fig. 3C). Quartz gangue hosting hematite lamellae is macroscopically red.

The SEM-BSE images of enargite/luzonite grains (Fig. 4) show different shades of grey, which correlates with chemical heterogeneity of enargite/luzonite represented mostly by As and Sb content variation. A faint zoning could be discerned locally along the grain border as well as an outer whitish rim (Fig. 4A). The enargite/luzonite-tennantite relationship is highlighted by a SEM-BSE image (Fig. 4B) that shows that enargite/luzonite is cut by a tennantite stringer that partly follows the chemical heterogeneity of enargite/luzonite or that created it. The enargite/luzonite grain from Figure 4C shows apparently minor shade variations. The numbers depicted in Figure 4 indicate the EPMA points discussed below.

ELECTRON MICROPROBE ANALYSIS

EPMA data were acquired for enargite/luzonite and associated sulphides and sulphosalts. EPMA data for **enargite/luzonite** are presented in Table 1 and show significant chemical variations. The enargite/luzonite analysed contains variable concentrations of As (ranging between 12.07 and 17.96 wt.%) and Sb (between 0.27 and 8.74 wt.%). The variable As/Sb ratios determine the various shades of grey in SEM-BSE images of enargite/luzonite (Fig. 4), i.e. the darker shades correspond to lower Sb content (#5–7; #11–14; 0.27 to 2.42 wt.%) and

Table 1

Representative EPMA results (in wt.%) for enargite/luzonite from the Cisma ore deposit (Băiuţ metallogenic field)

No.	1	2	3	4	5	6	7	8	9	10	11	12	13	14	Av.
Cu	47.41	47.5	47.89	47.80	48.25	47.90	48.39	47.11	47.50	47.19	47.50	46.93	47.44	47.67	47.61
Ag	0.00	–	0.00	–	–	–	–	0.00	0.00	–	–	0.30	–	–	–
Zn	0.00	0.00	0.00	0.00	0.00	0.00	0.00	0.00	0.00	0.00	0.37	0.67	–	0.00	0.07
Fe	0.37	0.26	0.19	0.22	0.54	1.32	0.53	0.25	0.29	0.29	1.43	1.32	2.61	2.29	0.85
As	12.92	14.35	14.17	15.30	16.68	16.55	16.91	12.52	13.20	12.07	16.31	16.17	17.96	17.71	15.20
Sb	6.15	6.08	5.94	4.84	2.10	2.04	1.65	8.74	7.17	8.38	2.42	2.20	0.27	0.27	4.16
S	34.57	32.24	32.33	32.51	32.55	32.75	33.18	31.98	32.53	32.68	32.12	32.29	32.85	32.39	32.64
Total	101.42	100.44	100.52	100.67	100.12	100.56	100.66	100.60	100.69	100.61	100.15	99.88	101.13	100.33	100.53*

The value marked with * represents the sum of the average value of the elements, while "–" represents values below the detection limit; the Pb, Mn, Cd, Sn contents are below the detection limit, while Bi was not detected

Table 2

Representative EPMA results (in wt.%) for tetrahedrite–tennantite, chalcopyrite and sphalerite

Mineral	tetrahedrite–tennantite					chalcopyrite	sphalerite		
Elements	tn1	tn2	tn3	tn4	average	1	1	2	average
Cu	43.99	44.70	43.36	43.81	43.97	34.55	0.21	0.32	0.27
Ag	0.60	0.35	0.54	0.58	0.52	0.00	0.00	–	0.00
Zn	–	0.00	0.08	0.00	–	0.00	62.77	61.94	62.36
Fe	6.33	5.70	8.15	6.49	6.67	30.64	2.62	3.21	2.92
Pb	0.78	0.54	–-	0.61	0.48	0.00	0.00	–	0.00
As	18.02	17.91	15.48	18.10	17.38	0.00	0.02	0.02	0.02
Sb	1.73	2.14	3.12	1.67	2.17	0.00	0.00	0.00	0.00
Cd	0.06	–-	0.10	0.06	0.06	0.00	0.61	0.64	0.63
Mn	0.00	0.00	0.00	–	0.00	–	0.06	0.08	0.07
S	28.82	28.86	28.03	28.82	28.63	35.26	34.05	34.54	34.30
Total	100.33	100.20	98.86	100.14	99.88	100.45	100.34	100.75	100.55

"–" represents values below the detection limit

the lighter shades correspond to higher Sb content (#8–10; 7.17 to 8.74 wt.%). The calculated average chemical formula of enargite/luzonite is $(Cu_{2.97},Fe_{0.06},Zn_{0.004})_{=3.03}(As_{0.80},Sb_{0.14})_{=0.94}S_{4.03}$.

The acquired EPMA data for minerals from the **tetrahedrite–tennantite** series (Table 2) show higher average values for As (17.38 wt.%) than for Sb (2.17 wt.%), with chemical compositions ranging between 15.48–18.10 wt.% (As), and 1.67–3.12 wt.% (Sb), respectively (Table 2). The mineral grains analysed are closer to tennantite composition. Silver is commonly present in tennantite with values ranging from 0.35 to 0.60 wt.% (Table 2). Overall, a higher Fe content correlates well to higher Sb amount. The calculated average chemical formula of tennantite is $(Cu_{10.22},Fe_{1.76},Ag_{0.07},Pb_{0.05},Cd_{0.01})_{=12.11}(Sb_{0.26},As_{3.43})_{=3.69}S_{13.20}$.

The EPMA data on **chalcopyrite** reveals almost ideal Cu, Fe, and S values (Table 2). The calculated chemical formula of the analysed chalcopyrite grain is $Cu_{0.99}Fe_{1.00}S_{2.01}$.

The **sphalerite** analysed (Table 2), contains less than 4.2 wt.% of all minor metals replacing Zn, i.e. (in wt.%), Fe (min = 2.62; max = 3.21); Cd (min = 0.61; max = 0.64); Cu (min = 0.21; max = 0.32), and Mn (min = 0.06; max = 0.08). The average chemical formula of the sphalerite is $(Zn_{0.91},Cu_{0.004},Fe_{0.05},Cd_{0.01},Mn_{0.001},As_{0.0003})_{=0.97}S_{1.03}$.

X-RAY POWDER DIFFRACTION

Whitish-yellow alteration minerals deposited in voids within enargite-bearing ore from Cisma were separated for XRD analyses from the sample shown in Figure 2A. The XRD data confirms the presence of kaolinite, calcite and galena.

An ore sample from Herja held by the County Museum of Mineralogy "Victor Gorduza", Baia Mare, Romania labeled "quartz–enargite" was also investigated (Fig. 2C). The specimen is composed of 0.5–1 cm long greyish-black prismatic crystals with metallic luster (Fig. 2D) associated with pyrite and quartz. The XRD of the prismatic metallic crystals confirms the occurrence of enargite and the minor presence of tennantite and galena.

DISCUSSION

Enargite/luzonite–famatinite occurrences in Romania are minor. Several examples are known from the Apuseni Mountains in compatible well-documented ore deposit environments, e.g., the Pârâul lui Avram HS deposit (Socolescu et al., 1963), the Roşia Poieni Cu-Au porphyry and overprinting HS veins, and HS veins overprinting Bucium-Tarniţa Cu-Au porphyry (Cioacă et al., 2014). Enargite, famatinite and luzonite are only briefly mentioned in the Baia Mare metallogenic district (cf. Pomârleanu, 1971; Petrulian et al., 1976; Bailly et al., 1998) without any analytical data or geological information on the ore deposit context.

SEM-BSE images and EPMA data on enargite/luzonite grains indicate rarely homogeneous (Fig. 4C) and more frequently heterogeneous (Fig. 4A, B) compositions due mostly to variable Sb and As contents (Table 1). The optical microscopy study on the ore samples available from Cisma did not allow clear discrimination between enargite and famatinite. However, as shown in Figure 5, the composition of the mineral grains analysed indicates intermediate phases closer to enargite/luzonite.

Optical microscopy distinction between enargite and luzonite is uncertain (Uytenbogaardt and Burke, 1971; Pracejus, 2015), and their ideal chemical composition is also identical. Based on high-resolution transmitted electron microscopy and electron diffraction on selected areas in samples from the Recsk porphyry-HS system (NE Hungary), Pósfai and Sundberg (1998) demonstrated that enargite and luzonite are commonly intergrown at the atomic level. However, Springer (1969) has shown that the maximum content of Sb in enargite

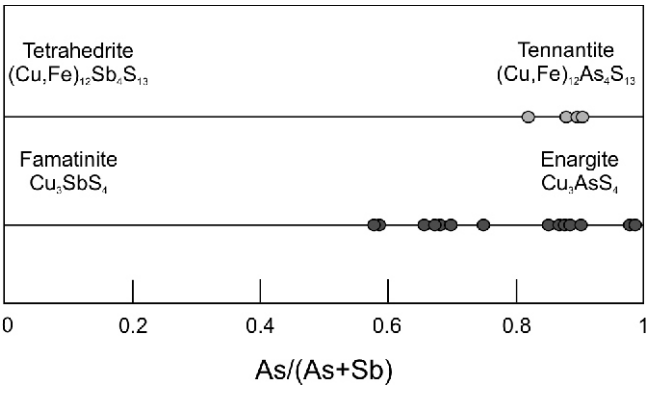

Fig. 5. Plot of compositional variations of analysed enargite/luzonite and tennantite from Cisma in the diagram of Ciobanu et al. (2005)

can reach up to 6 wt.%, and Gaines (1957) demonstrated by XRD and chemical data that there is a complete solid solution between luzonite and famatinite. Consequently, certain distinction between enargite and luzonite can be made based on microchemical data only if the Sb content exceeds the limit highlighted by Springer (1969), i.e. 6 wt.% Sb that corresponds to ~20 mol % Cu_3SbS_4. Among the available EPMA results acquired from Cisma there are three compositions exceeding this Sb limit (Table 1), i.e. #8 (8.74 wt.%), #9 (7.17 wt.%), and #10 (8.38 wt.%), three other points are close to the limit, i.e. #1 (6.15 wt.%), #2 (6.08 wt.%), and #3 (5.94 wt.%), and the remaining ones are largely below. The EPMA points #8–10 thus indicate the occurrence of luzonite, which likely corresponds to the lighter spots in Figure 4A. The Sb values of the EPMA points #1–3 are too close to the limit (6 wt.%) to really discriminate between enargite and luzonite, and the remaining EPMA points did not support such discrimination. Pósfai and Buseck (1998) stated that when enargite and luzonite coexist, luzonite typically contains more Sb than enargite. Moreover, the same authors suggest that enargite that coexists with luzonite-famatinite can contain a maximum of 11 mol% Cu_3SbS_4, which corresponds approximately to 3.3 wt.% Sb. However, higher values were encountered for enargite associated with Mn-bearing tetrahedrite. According to these additional observations, the EPMA points #1–4 with Sb content ranging from 4.84 to 6.15 represent luzonite, and the remaining EPMA points #5–7 and #11–14 with Sb content ranging from 0.27 to 2.42 (Table 1) correspond to enargite. A similar Sb content range in enargite was reported by Deyell and Hedenquist (2011) from the Lepanto high-sulphidation Cu-Au deposit and the nearby Far Southeast Cu-Au porphyry deposit, Mankayan district, Philippines, i.e., 0.19 to 3.59 wt.% Sb.

EPMA and LA-ICP-MS studies of trace elements in enargite from porphyry and HS ores in the Far Southeast and Lepanto deposits, Philippines reveal Ag, Fe and Pb enrichment in enargite from the main HS ore body (Deyell and Hedenquist, 2011). The Fe content in enargite from Cisma, i.e., up to 2.61 wt.%, exceeds the maximum Fe content reported from the Lepanto main ore body that ranges from 0.21 to 0.75 wt.%. As regards the enargite from Cisma, the EPMA detection limits are too high for the identification of Pb and Ag contents in enargite as reported by Deyell and Hedenquist (2011), performed by LA-ICP-MS, and consequently it is impossible to propose other correlations. Based on EPMA and LA-ICP-MS data on enargite from porphyry, HS and IS ore deposits from the Zijinshan Cu-Au ore district (southeastern China), Liu et al. (2019) have shown that the trace element pattern of enargite is specific for each deposit type and for the case of epithermal deposits it correlates to the transition from HS to IS and reflects the hydrothermal fluid evolution. The enargite from Cisma shows similar depletion in Zn as does the enargite from the Longjiangting IS deposit (Liu et al., 2019), and enrichment in Sb and Fe as in the IS enargite rim formed on enargite from the Wuziqilong Cu deposit (Liu et al., 2019). Overall, these authors stated that at least for the Zijinshan ore district in China, enargite from HS deposits is enriched in Te and Sn, and enargite from IS deposits is depleted in these elements and enriched in Sb and Se. Accordingly, the trace element chemical pattern of enargite from Cisma (Table 1), e.g., Sn below the detection limit and enrichment in Sb, suggests its IS affinity.

The optical microscopy study of the Cisma ores shows that hematite predated the sulphides and chalcopyrite is partly replaced by enargite/luzonite, which is cut and partly replaced by tennantite (Figs. 3D and 4C). Hematite was previously identified in the paragenesis of Văratec ore deposit, Băiuţ metallogenic field as mentioned by Costin and Vlad (2005) in the first two mineralization stages, i.e., quartz–Fe-oxides±pyrite±wolframates (1), and quartz–chalcopyrite–Bi-minerals–pyrite±Fe-oxides (2). The widespread occurrence of hematite in the ore samples from Cisma indicates an intermediate sulphidation stage according to the log $f(S_2)$ – temperature diagram of Einaudi et al. (2003).

These mineral relationships, indicating the paragenetic sequence hematite–chalcopyrite–enargite and luzonite–tennantite, suggest an early intermediate sulphidation environment (hematite and chalcopyrite) followed by a passage towards high-sulphidation conditions as indicated by chalcopyrite replacement by enargite/luzonite and a final overprint by an intermediate sulphidation stage suggested by enargite/luzonite replacement by tennantite and the absence of bornite and pyrite. Similar sulphidation state evolution trend was found in the Recsk porphyry–skarn–epithermal metallogenic system, Hungary, by Takács et al. (2017). The abundant hypogene kaolinite closely related to the enargite–tennantite–chalcopyrite mineral assemblage indicates the intermediate/high sulphidation state. Similarly, the presence of significant enargite associated with tennantite and galena in the sample studied from the Herja ore deposit suggests a similar intermediate/high sulphidation environment during ore deposition.

Based mostly on LA-ICP-MS data on enargite from enargite-rich HS ore bodies, Deyell and Hedenquist (2011) showed a lateral variation of trace elements in enargite from porphyry to proximal (HS) and distal (IS) environments. This variability is characterized by: Au and Te enrichment proximal to cogenetic porphyry; Ag, Fe, and Pb enrichment in the main HS ore body; and Zn±Cd enrichment in distal veins. Thus, the chemical character of the enargite could be used as a vectoring tool for exploration in porphyry to epithermal environments. The occurrence of $Cu_3(As,Sb)S_4$ minerals (enargite and luzonite) in the Cisma and Herja ore deposits suggests that IS and HS conditions existed during the formation of these deposits. Strongly leached and highly silicified zones, e.g., massive and vuggy silica hosted by rocks with argillic/advanced argillic alteration halos and containing disseminated mineralization, were ignored in the Baia Mare district. Similarly, the presence of porphyry deposits was generally neglected. An overview of the ore deposits from the Baia Mare metallogenic district using up-to-date ore deposit models based on available geological and mineralogical data, as proposed by Nieć et al. (2016) for the Polish Carpathians, could reveal prospective spots at least for HS style ores.

The common sulphides have been previously described from all ore deposits within the Băiuţ metallogenic field. Galena was identified in the upper part of the veins from the Cisma–Poiana Botizei deposit (Damian et al., 2010) and from the dominantly Pb-rich Văratec ore deposit, being associated with sphalerite and subordinate chalcopyrite (Cook, 1998).

The sphalerite analysed has similar amounts of Fe (2.62 and 3.21 wt.% Fe) as the sphalerite-1 described by Plotinskaya et al. (2014), characterized by low Fe content (1.3 to 4.6 wt.%). However, the sphalerite analysed has lower Mn (0.06–0.08 wt.%) and higher Cd (0.61–0.64 wt.%) contents as compared to the sphalerite-1 (cf. Plotinskaya et al., 2014), i.e. 0.5–0.7 wt.% Mn and 0.2 wt.% Cd, respectively. Similarly, chalcopyrite inclusions have been described in the zoned sphalerite-2 from the Cisma vein reported by Plotinskaya et al. (2012). Previous studies on the Baia Mare metallogenic district (Bailly et al., 1998) and the Văratec ore deposit (Costin, 2003; Costin and Vlad, 2005) interpreted chalcopyrite as part of the second paragenetic sequence, associated with quartz, Fe-oxides, pyrite and Bi-minerals.

The tennantite grains analysed (Table 2) have As *apfu* >3 (As *apfu* ranging between 3.09–3.56, average 3.43), as compared to tennantite–tetrahedrite with As *apfu* <2.2 from Băiuţ

reported by Damian and Damian (2003). The variation of As and Sb content in the tennantite grains analysed is shown in Figure 5. According to Damian and Damian (2003) the ore deposits from the Baia Mare area contain Zn-rich tetrahedrites and Fe-rich tennantites, with up to 7.69 wt.% Zn and 6.46 wt.% Fe, respectively. However, only one out of 4 tennantite grains analysed in the present study contains Zn (0.08 wt.%) close to the detection limit (0.065 wt.%), while all the grains analysed have high Fe values, ranging from 5.70 to 8.15 wt.%, exceeding the upper limit previously mentioned.

The tennantite from Cisma has high Fe (ranging from 5.70 to 8.15 wt.%), low Zn (from below the detection limit up to 0.8 wt.%), no Mn and a clear Cu-excess with Cu >10 *apfu* (Table 2 and Fig. 4C). Manganese-free fahlore minerals were reported by Takács et al. (2017) from the Lahóca Hill, Recsk ore complex, Hungary, from pre- and post-enargite depositional stages in HS ore bodies. Contrastingly, fahlore minerals containing Mn were identified by the same authors in the Lejtanka transitional HS-IS and Parád IS deposits from the Recsk ore complex, Hungary, and these geochemical peculiarities were considered evidence of lower sulphidation state hydrothermal fluids, likely responsible for IS mineralization. Consequently, the absence of Mn in tennantite from Cisma could be also interpreted as an indicator of the HS character of the host ore. The Ag content of tennantite from Cisma (0.35–0.60 wt.%) is in agreement with the previously reported data by Damian and Damian (2003), which stated that the Ag content in tetrahedrite-tennantite from the Baia Mare district is <2 wt.%.

CONCLUSIONS

EPMA results acquired from the Cisma ore deposit in the Băiuţ ore field and XRD data on an ore sample from the Herja ore deposit represent the first analytical evidence for the occurrence of enargite and luzonite in the Baia Mare ore district. The newly acquired micro-chemical results on enargite/luzonite, sphalerite and tennantite, and the significant occurrence of kaolinite, reveal a clear intermediate to high sulphidation state environment of Cu-rich ore at Cisma. An evolution trend of the sulphidation state of the hydrothermal fluids is inferred for Cisma from an early IS stage with hematite and chalcopyrite to a HS stage with enargite and luzonite and a final IS stage with tennantite and base metal sulphides.

The hitherto generally accepted low sulphidation character of the Neogene Baia Mare metallogenic district should be reconsidered from these results, and this approach may open new mineral exploration challenges for IS/HS ores and their deep/hidden porphyry roots in this district. The massive and/or vuggy silica bodies hosted by argillic/advanced argillic alteration with disseminated Au mineralization seem to represent a new exploration target in the Baia Mare metallogenic district.

Acknowledgments. Many thanks to I. Denuţ , director of the "Victor Gorduza" County Mineralogical Museum of Baia Mare for providing access to the ore sample collection of the museum and permission to sample the enargite specimen from the Herja ore deposit. Thanks are addressed to D. Béziat (GET Toulouse) for granting access to ore microscopy facilities. T. Aigouy (GET Toulouse) and P. de Parseval (UMS 3623 – Centre de MicroCaractérisation Raimond Castaing, Toulouse) for assistance during SEM and EPMA sessions. The XRD device from the Department of Geology, Babeş-Bolyai University, Cluj-Napoca used for this work was acquired in the framework of the RICI/INIR program with the financial support of PNCDI II (2007–2013). The review made by P. Lattanzi and an anonymous reviewer and the suggestions offered by S. Oszczepalski greatly improved the quality of the manuscript.

REFERENCES

András, K., 2017. Studiul mineralogic al minereurilor din perimetrul Băiuţ (judeţul Maramureş), cu privire specială asupra zăcămintelor Văratec, Cisma, Coasta Ursului, Johan Hell, Breiner şi Poiana Botizei (in Romanian). Unpublished Master thesis, University Babeş-Bolyai, Cluj-Napoca.

Bailly, L., Milési, J.P., Leroy, J., Marcoux, E., 1998. The Au-Cu-Zn-Sb epithermal mineralisations of the Baia Mare district (North Romania): new mineralogical and microthermometric results (in French with English summary). Académie des Sciences, Géomatériaux, Paris, **327**: 385–390.

Borcoş, M., 1994. Neogene volcanicity/metallogeny in the Oaş-Gutâi Mts. In: Field trip guide IGCP 356, Bucharest: Plate Tectonics and Metallogeny in the East Carpathians and Apuseni Mts. (eds. M. Borcoş and Ş. Vlad): 20–22.

Borcoş, M., Gheorghiţă, I., 1976. Neogene hydrothermal ore deposits in the volcanic Gutâi Mountains. IV. Băiuţ-Văratec-Botiza metallogenic field. Revue Roumaine de Géologie, Géophysique et Géographie, Série de Géologie, **20**: 197–209.

Cădere, D., 1925. Fapte pentru a servi la descrierea mineralogică a României (in Romanian). Academy of Romania, Memoriile Secţiunii Ştiinţifice, **3**.

Cioacă, E.M., Munteanu, M., Qi, L., Costin, G., 2014. Trace element concentrations in porphyry copper deposits from Metaliferi Mountains, Romania: a reconnaissance study. Ore Geology Reviews, **63**: 22–39.

Ciobanu, C.L., Cook, N.J., Capraru, N., Damian, G., Cristea, P., 2005. Mineral assemblages from the veins salband at Săcărâmb, Golden Quadrilateral, Romania: I. Sulphides and sulphosalts. Geochemistry, Mineralogy and Petrology, **45**: 47–55.

Cook, N.J., 1998. Bismuth sulphosalts from hydrothermal vein deposits of Neogene Age, N.W. Romania. Mitteilungen der Österreichische Mineralogische Gesselschaft, **143**:19–39.

Cook, N.J., Damian, G.S., 1997. New data on "plumosite" and other sulphosalt minerals from the Herja hydrothermal vein deposit, Baia Mare district, Rumania. Geologica Carpathica, **48**: 387–399.

Costin, D., 2003. Compositional data on bournonite–$CuPbSb_3$ from Văratec ore deposit, Băiuţ mine field, Eastern Carpathians, Romania. Studia Universitatis Babeş-Bolyai, Geologia, **48**:45–54.

Costin, D., Vlad, Ş., 2005. Ore formation at Văratec–Băiuţ, Baia Mare region, East Carpathians, Romania. Geochemistry, Mineralogy and Petrology, **43**: 64–68.

Crahmaliuc, R., Andrei, J., Crahmaliuc, A., 1995. The magnetic modeling of the Gutâi Neogene plutonic body. Romanian Journal of Stratigraphy, **76**: 63–64.

Csontos, L., 1995. Tertiary tectonic evolution of the Intra-Carpathian area: a review. Acta Vulcanologica **7**:1–15.

Csontos, L., Nagymarosy, A., 1998. The Mid-Hungarian Line: a zone of repeated tectonic inversions. Tectonophysics, **297**: 51–71.

Csontos, L., Nagymarosy, A., Horváth, F., Kovacs, M., 1992. Tertiary evolution of the Intra-Carpathian area: a model. Tectonophysics, **208**: 221–241.

Damian, G.Ş., 1996. Studiul mineralogic, geochimic şi genetic al zăcământului polimetalic de la Herja (in Romanian). Unpublished Ph.D. thesis, University of Bucharest, Romania.

Damian, F., Damian, G., 2004. Mineral paragenesis of the hydrothermal ore deposits from Baia Mare area Romania. Scientific Bulletin of North University Centre of Baia Mare, Series D, Mining, Mineral Processing, Non-ferrous Metallurgy, Geology and Environmental Engineering, **18**: 155–172.

Damian, G., Damian, F., 2003. Comparative study of the tetrahedrites from the Metaliferous Mts. and Baia Mare district (Romania) based on microprobe analyses. Studia Universitatis Babeş-Bolyai, Seria Geologia, Special Issue: 27–29.

Damian, G., Nedelcu, L., Istvan, D., 1995. Two representative vein deposits (Au-Ag and Pb-Zn) related to Neogene volcanic structures. Romanian Journal of Mineralogy, **77**: 45–63.

Damian, G., Damian, F., Kovalenker, V., Plotinskaya, O.Y., 2010. Native bismuth and bismuth sulphosalts in Cisma Poiana Botizei mineralizations, Baia Mare District. Analele Stiintifice ale Universităţii. Al. I. Cuza din Iaşi, Geologie: 189–191.

Damian, G., Damian, F., Konečný, P., Kollárová, V., 2016. A new occurrence of wolframite-ferberite in Romania. Romanian Journal of Mineral Deposits, **89**: 49–54.

Deyell, C.L., Hedenquist, J.W., 2011. Trace element geochemistry of enargite in the Mankayan district, Philippines. Economic Geology, **106**: 1465–1478.

Edelstein, O., Bernád, A., Kovacs, M., Crihan, M., Pécskay, Z., 1992. Preliminary data regarding the K-Ar ages of some eruptive rocks from Baia Mare Neogene volcanic zone. Revue Roumaine de Géologie, Géophysique et Géographie, Série de Géologie, **36**: 45–60.

Einaudi, M.T., Hedenquist, J.W., Inan, E.E., 2003. Sulfidation state of fluids in active and extinct hydrothermal systems: transition from porphyry to epithermal environments. SEG Special Publication, **10**: 283–313.

Fodor, L., Csontos, L., Bada, G., Györfi, I., Benkovics, L., 1999. Cenozoic tectonic evolution of the Pannonian basin system and neighboring orogens: a new synthesis of paleostress data. Geological Society Special Publications, **156**: 295–334.

Fülöp, A., 2001. Analiza secvenţială a piroclastitelor acide din baza complexului vulcanic al Munţilor Gutâi; reconstituiri paleovulcanice şi paleosedimentologice (in Romanian). Ph.D. thesis, University of Bucharest.

Fülöp, A., 2003. Debutul vulcanismului în Munţii Gutâi. Reconstituiri paleovulcanologice şi paleosedimentologice (in Romanian). Dacia Publishing House, Cluj-Napoca.

Fülöp, A., Kovacs, M., 2003. Petrology of Badenian ignimbrites, Gutâi Mts. (Eastern Carpathians). Studia Universitatis Babeş-Bolyai, Geologia., **48**:17–28.

Gaines, R.V., 1957. Luzonite, famatinite and some related minerals. American Mineralogist, **42**: 766–779.

Giuşcă, D., 1960. Adularizarea vulcanitelor din regiunea Baia Mare (in Romanian). Studii şi Cercetări de Geologie, Geografie, Seria Geologia, **5**: 499–507.

Grancea, L., Bailly, L., Leroy, J., Banks, D., Marcoux, E., Milesi, J.P., Cuney, M., Andre, A.S., Istvan, D., Fabre, C., 2002. Fluid evolution in the Baia Mare epithermal gold/polymetallic district, Inner Carpathians, Romania. Mineralium Deposita, **37**: 630–647.

Gurău, A., Roşu, N., Bălaşa, E., Bordea, R., 1970. Considerations regarding the structure and genesis of the Borzaş ore deposit (Baia Mare). Dări de Seamă ale Şedinţelor Institutului Geologic, **56** (2 for 1968–1969): 27–48.

Hedenquist, J.W., Matsuhisa, Y., Izawa, E., White, N.C., Giggenbach, W.F., Aoki, M., 1994. Geology, geochemistry, and origin of high sulfidation Cu-Au mineralization in the Nansatsu district, Japan. Economic Geology, **89**: 1–30.

Huismans, R.S., Podladchikov, Y.I., Cloething, S., 2001. Dynamic modelling of the transition from passive to active rifting, application to the Pannonian Basin. Tectonics, **20**: 1021–1039.

Iancu, O.G., Kovacs, M., 2010. Ore deposits and other classic localities in the Eastern Carpathians: From metamorphics to volcanics. Acta Mineralogica-Petrographica, Field Guide Series, **19**: 1–55.

Iştvan, D., Vârşescu, I., Halga, S., Grancea, L., 1995. Gold-silver epithermal levels and associations in the eastern area of the Gutâi Mts. and in the Văratec Mts. (Firiza-Botiza area), East Carpathians, Romania. Studia Universitatis Babeş-Bolyai, Geologia, **40**: 195–210.

Kouzmanov, K., Bailly, L., Tămaş, C., Ivăşcanu, P., 2005. Epithermal Pb-Zn-Cu(Au) deposits in the Baia Mare district, Eastern Carpathians, Romania. Ore Geol. Reviews, **27**: 48–49.

Kovacs, M., Fülöp, A., 2003. Neogene volcanism in Gutâi Mts. (Eastern Carpathians): a review. Studia Universitatis Babeş-Bolyai, Geologia, **48**: 3–16.

Kovacs, M., Fülöp A., 2010. Baia Mare metallogenetic district. Acta Mineralogica-Petrographica, Field Guide Series, **19**: 5–13.

Kovacs, M., Edelstein, O., Gabor, M., Bonhomme, M., Pécskay, Z., 1997. Neogene magmatism and metallogeny in Oaş-Gutâi-Ţibleş Mts.; a new approach based on radiometric datings. Romanian Journal of Mineral Deposits, **78**: 35–45.

Kovacs, M., Seghedi, I., Yamamoto, M., Fülöp, A., Pécskay, Z., Jurje, M., 2017. Miocene volcanism in the Oaş-Gutâi Volcanic Zone, Eastern Carpathians, Romania: relationship to geodynamic processes in the Transcarpathian basin. Lithos, **294–295**: 304–318.

Kovács, R., Tămaş, C.G., 2017. Cu-sulfosalts in Băiuţ metallogenetic field, Baia Mare district, Gutâi Mountains–preliminary scanning electron microscopy data (in Romanian). Volumul Sesiunii Ştiinţifice „Ion Popescu Voiteşti", Universitatea Babeş-Bolyai Cluj Napoca, Departamentul de Geologie: 24–30.

Kovács-Pálffy, P., Paulini, P., Răduţ, M., Cioroianu, V., 1977. Alunitizarea din Valea Brada, Negreşti Oaş (Munţii Gutâi) (in Romanian). Studii tehnice şi economice, **11**: 205–221.

Lang, B., 1979. The base metals-gold hydrothermal ore deposits of Baia Mare, Romania, Economic Geology, **74**: 1336–l351.

Lang, B., Edelstein, O., Steinitz G., Kovacs M., Halga S., 1994. Ar-Ar dating of adularia – a tool in understanding genetic relation between volcanism and mineralization: Baia Mare area (Gutâi Mountains), Northwestern Romania. Economic Geology, **89**: 174–180.

Liu, W., Cook, N.J., Ciobanu, C.L., Gilbert, S.E., 2019. Trace element substitution and grain-scale compositional heterogeneity in enargite. Ore Geology Reviews, **111**: 103004.

Manilici, V., Giuşcă, D., Stiopol, V., 1965. Studiului zăcământului de la Baia Sprie (Reg.Baia Mare) (in Romanian). Memorii, **7**: 1-95.

Marcoux, E., Grancea, L., Lupulescu, M., Milési, J.P., 2002. Lead isotope signatures of epithermal and porphyry-type ore deposits from the Romanian Carpathian Mountains. Mineralium Deposita, **37**: 173–184.

Mariaş, F., 1996. Câmpul metalogenetic Cavnic. Caracterizare geostructurală şi petrometalogenetică (in Romanian). Ph.D. thesis, University Babeş-Bolyai, Cluj-Napoca.

Mariaş, F., 2005. Metalogeneza districtului minier Baia Mare. Model bazat pe sistemul hidrotermal Cavnic (Maramureş). Evaluări comparative cu alte sisteme epitermale din lume (in Romanian). Editura Cornelius.

Márton, E., Pogac, P., Tunyi, I., 1992. Paleomagnetic investigations on Late Cretaceous-Cenozoic sediments from the NW part of the Pannonian Basin. Geologica Carpathica, **43**: 363–369.

Mârza, I., 2002. Geneza zăcămintelor de origine magmatică. 4. Metalogenia hidrotermală (in Romanian). Presa Universitară Clujeană.

Mârza, I., Tămaş, C.G., Tetean, R., Andreica, A., Denuţ, I., Kovács, R., 2019. Epithermal bicolor black and white calcite spheres from Herja ore deposit, Baia Mare Neogene ore district, Romania-genetic considerations. Minerals, **9**: 352.

Neubauer, F., Lips, A., Kouzmanov, K., Lexa, J., Ivăşcanu, P., 2005. Subduction, slab detachment and mineralization: the Neogene in the Apuseni Mountains and Carpathians. Ore Geology Reviews, **27**: 13–44.

Nieć, M., Radwanek-Bąk, B., Lenik, P., 2016. Outline of metallogeny of the Polish Carpathians – Ore deposit models and the possibility of discovery hidden ore deposits. Biuletyn Państwowego Instytutu Geologicznego, **467**: 9–40.

Panaiotu, C., Pécskay, Z., Panaiotu, C., 1996. Which is the time of rotation? Review of paleomagnetic and K-Ar data from Romania. Mitteilungen Gesellschaft der Geologie und Bergbaustudenten, **41**: 125.

Pătraşcu, S., Panaiotu, C., Şeclăman, M., Panaiotu, C.E., 1994. Timing of rotational motion of Apuseni Mountains (Romania): paleomagnetic data from Tertiary magmatic rocks. Tectonophysics, **233**:163–176.

Petrulian, N., Steclaci, L., Jude, R., Ştefan, H., Popescu, R., Cioran, A., 1976. Contributions to the metallogenesis and geochemistry of the Cavnic vein area. Révue Roumaine de Géologie, Géophysique et Géographie, Série de Géologie, **20**: 157–167.

Pécskay, Z., Lexa, J., Szakács, A., Seghedi, I., Balogh, K., Konecny, V., Zelenka, T., Kovacs, M., Póka, T., Fülöp, A., Márton, E., Panaiotu, C., Cvetkovic, V., 2006. Geochronology of Neogene magmatism in the Carpathian arc and intra-Carpathian area. Geologica Carpathica, **57**: 511–530.

Plotinskaya, O.Y., Prokofiev, V.Y., Damian, G., Damian, F., Lehmann, B., 2012. The Cisma deposit, Băiuţ district, Eastern Carpathians, Romania: sphalerite composition and formation conditions. Carpathian Journal of Earth and Environmental Sciences, **7**: 265–273.

Plotinskaya, O.Y., Damian, G., Damian, F., 2014. Sphalerite composition in the Baia Mare region, Eastern Carpathians, Romania (preliminary data). Romanian Journal of Mineral Deposits, **87**: 87–90.

Pomârleanu, V.V., 1971. Geotermometria şi aplicarea ei la unele minerale din România (in Romanian). Editura Academiei Republicii Socialiste România.

Pósfai, M., Buseck, P., 1998. Relationships between microstructure and composition in enargite and luzonite. American Mineralogist, **83**: 373–382.

Pósfai, M., Sundberg, M., 1998. Stacking disorder and polytypism in enargite and luzonite. American Mineralogist, **83**: 365–372.

Pracejus, B., 2015. The Ore Minerals under the Microscope. An Optical Guide. 2nd edition, Elsevier.

Rădulescu, D., Dimitrescu, R., 1965. Topografia mineralogică a României (in Romanian). Editura Academiei Republicii Socialiste România.

Săndulescu, M., 1984. Geotectonica României (in Romanian). Editura Tehnică.

Săndulescu, M., Russo-Săndulescu, D., 1981. Geological map of Romania, 1:50 000, sheet 19c. Institutul de Geologie şi Geofizică, Bucureşti.

Săndulescu, M., Visarion, M., Stanica, D., Stanica, M., Atanasiu, L., 1993. Deep structure of the inner Carpathians in the Maramures-Tisa zone (East Carpathians). Romanian Journal of Geophysics, **16**: 67–76.

Seghedi, I., Balintoni, I., Szakács, A., 1998. Interplay of tectonics and Neogene post-collisional magmatism in the Intracarpathian area. Lithos, **465**: 483–499.

Seghedi, I., Downes, H., Harangi, S., Mason, P.R.D., Pécskay, Z., 2005. Geochemical response of magmas to Neogene-Quaternary continental collision in the Carpathian Pannonian region: a review. Tectonophysics, **410**: 485–499.

Seghedi, I., Downes, H., 2011. Geochemistry and tectonic development of Cenozoic magmatism in the Carpathian–Pannonian region. Gondwana Research, **20**: 655–672.

Socolescu, M., Bonea, L., Haiduc, P., 1963 Contribuţii la cunoaşterea mineralizaţiei cuprifere de la Pârâul lui Avram (Munţii Apuseni) (in Romanian). Revista Minelor **14**: 393–402.

Springer, G., 1969. Compositional variations in enargite and luzonite. Mineralium Deposita, **4**: 72–74.

Stanciu, C., 1973. Hydrothermal alteration of Neogene volcanics rocks from ore deposits in Gutâi Mountains (East Carpathians). Revue Roumaine de Géologie, Géophysique et Géographie, Série de Géologie, **17**: 43–62.

Stanciu, C., 1984. Hypogene alteration genetic types related to the Neogene volcanism of the East Carpathians, Romania. Anuarul Institutului de Geologie si Geofizică, **44**: 235–244.

Szabó, C., Harangi, S., Csontos, L., 1992. Review of Neogene and Quaternary volcanism of the Carpathian–Pannonian region. Tectonophysics, **208**:243–256.

Takács, A., Molnár, F., Turi, J., Mogessie, A., Menzies, J.C., 2017. Ore mineralogy and fluid inclusion constraints on the temporal and spatial evolution of a high-sulfidation epithermal Cu-Au-Ag deposit in the Recsk ore complex, Hungary. Economic Geology, **112**: 1461–1481.

Takéuchi, Y., Sadanaga, R., 1969. Structural principles and classification of sulfosalts. Zeitschrift für Kristallographie, **130**: 346–368.

Tămaş, C.G., Har, N., Mârza, I., Denuţ, I., 2018. The black calcite and its mineral assemblage in Herja ore deposit, Romania. European Journal of Mineralogy, **6**: 1141–1153.

Tischler, M., Gröger, H.R., Fügenschuh, B., Schmid, S.M., 2007. Miocene tectonics of the Maramureş area (Northern Romania): implications for the Mid-Hungarian fault zone. International Journal of Earth Sciences, **96**: 473–496.

Udubaşa, G., Ilinca, G., Marincea, Ş., Săbău, G., Rădan, S., 1992. Minerals in Romania: the state of the art 1991. Romanian Journal of Mineralogy, **75**: 1–51.

Udubaşa, G., Szakáll, S., Duda, R., Kvasnytsya, V., Koszowska, E., Novak, M., 2002. Minerals of the Carpathians. Granit Publishing House, Prague, Czech Republic.

Uytenbogaardt, W., Burke, E.A.J., 1971. Tables for microscopic identification of ore minerals. 2nd ed., Elsevier, Amsterdam.